Average-Value Modeling of Synchronous Machine Line-Commutated Converter using a Constant-Parameter Voltage-Behind-Reactance Interfacing Circuit

H. Atighechi, S. Amini Akbarabadi, F. Therrien, J. Jatskevich

***Abstract*— Average-Value Models (AVMs) are becoming increasingly important in system-level studies of modern energy grid systems wherein many power–electronic-based components are found. In this paper, a new and improved analytical AVM of the synchronous machine/rectifier system is developed. As opposed to previously developed models, the proposed approach does not contain algebraic loops and is therefore numerically more efficient. The approach encompasses a recently proposed voltage-Behind-Reactance (VBR) machine model with constant parameters, which allows direct and efficient interfacing between the machine and rectifier sub-models. The proposed AVM has been implemented in MATLAB/Simulink, and is verified against the original detailed switching system.**

***Keywords*: Average-value model, , rectifier, synchronous machine, voltage-behind-reactance formulation.**

I. Introduction

Since the need for system-level modeling and analysis tools is rapidly increasing, the average-value modeling approach [1]-[14] has been recognized as a powerful tool for studying and analyzing complicated power-electronic-based systems. Average-value models (AVMs) predict the steady-state and transient behavior of the original system for dynamics slower than the switching frequency. Because the effect of fast switching is averaged or neglected within a prototypical switching interval, the AVMs are computationally efficient and potentially can execute orders of magnitude faster than the corresponding detailed switching models. In addition, the AVMs are continuous and can therefore be linearized about any operating point for small-signal frequency-domain characterization.

The first analytical derivation of an AVM for a synchronous machine/line-commutated converter system was published in the late 1960s [1], and improved models have been developed ever since [2]-[8]. The most complete analytical AVM that is accurate in both time- and frequency-domains has been introduced in [7]. However, formulation [7] is implicit, which results in an algebraic loop when implementing the corresponding state-space model. Numerical iterations are thus required at each time step of the solution in order to solve the algebraic loop.

In this paper, an improved analytical AVM of the synchronous machine/rectifier system is proposed. The developed AVM is explicit (i.e. has no algebraic loops); hence, it is potentially significantly more efficient as no additional iterations are required. In this approach, the synchronous machine is modeled using a constant-parameter voltage-behind-reactance (VBR) formulation [15], [16], and the rectifier is modeled based on the analytical approach presented in [17]. In the proposed AVM formulation, the machine and rectifier sub-models are directly interfaced with constant parameters.

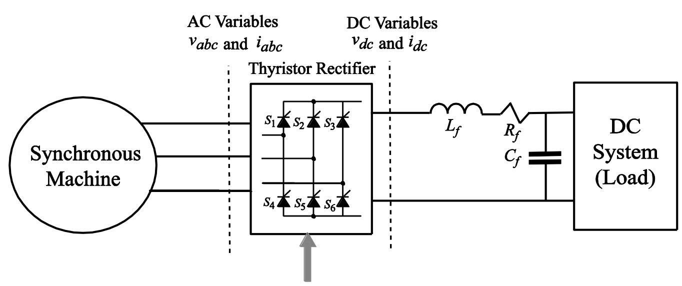

Fig. 1. Synchronous machine/rectifier system.

II. Voltage-Behind-Reactance (VBR) Machine Model

The proposed AVM contains a VBR synchronous machine model with constant parameters [15], which allows direct and constant interfacing between the machine and rectifier sub-models. In the method presented in [15] and [16], an artificial damper winding is added to the rotor circuit of the VBR model. This new winding eliminates dynamic saliency by equating the subtransient inductances L''_{mq} and L''_{md}, which in turn yields a constant-parameter equivalent stator circuit. This

---

This research was supported by the Natural Science and Engineering Research Council (NSERC) of Canada, under the Discovery Grant.

H. Atighechi, S. Amini Akbarabadi, F. Therrien and J. Jatskevich are with the Department of Electrical and Computer Engineering, University of British Columbia, Vancouver, BC, V6T 1Z4, Canada (e-mail: { hamida, sorousha, francist, jurij}@ece.ubc.ca).

Paper submitted to the International Conference on Power Systems Transients (IPST2013) in Vancouver, Canada July 18-20, 2013.

added winding should have a large enough resistance to avoid any impact on the low frequencies; however, it also shouldn't be too large in order not to significantly increase the numerical stiffness of the state-space model. Since, the subtransient inductance in the d-axis is typically the smallest [15], the additional winding is added to the q-axis.

Here, the rotor is considered to have M damper windings in the q-axis and N damper plus one field windings in the d-axis. Including the extra winding ($M+1$) in the q-axis, the voltage equation for the interfacing stator circuit, represented in the abc phase coordinates, is [15]

$$\mathbf{v}_{abcs} = r_s \mathbf{i}_{abcs} + L_D p \mathbf{i}_{abcs} + L_0 p(3\mathbf{i}_{0s}) + \mathbf{e}''_{abc}. \tag{1}$$

where

$$r_D = r_s, \tag{2}$$

$$L_D = L_{ls} + L''_{md}, \tag{3}$$

$$L_0 = -\frac{1}{3} L''_{md}. \tag{4}$$

The dynamic equations of the rotor subsystem are modeled in qd coordinates in the rotor reference frame [15]. The equivalent voltage source $\mathbf{e}''_{abc}$ is therefore computed by applying Park's inverse transformation [17] to the resulting qd subtransient voltages:

$$e''_q = \omega_r \lambda''_d + \sum_{j=1}^{M+1} \left(\frac{L''_{mq} r_{kqj}}{L^2_{lkqj}} (\lambda_{mq} - \lambda_{kqj}) \right), \tag{5}$$

$$e''_d = -\omega_r \lambda''_q + \sum_{j=1}^{N} \left(\frac{L''_{md} r_{kdj}}{L^2_{lkdj}} (\lambda_{md} - \lambda_{kdj}) \right) + \frac{L''_{md}}{L_{lfd}} v_{fd} + \frac{L''_{md} r_{fd}}{L^2_{lfd}} (\lambda_{md} - \lambda_{fd}). \tag{6}$$

where

$$L''_{mq} = \left(\frac{1}{L_{mq}} + \sum_{j=1}^{M+1} \frac{1}{L_{lkqj}} \right)^{-1}, \tag{7}$$

$$L''_{md} = \left(\frac{1}{L_{mq}} + \frac{1}{L_{lfd}} + \sum_{j=1}^{N} \frac{1}{L_{lkdj}} \right)^{-1}, \tag{8}$$

$$\lambda''_q = L''_{mq} \left(\sum_{j=1}^{M+1} \frac{\lambda_{kqj}}{L_{lkqj}} \right), \tag{9}$$

$$\lambda''_d = L''_{md} \left(\frac{\lambda_{fd}}{L_{lfd}} + \sum_{j=1}^{N} \frac{\lambda_{kdj}}{L_{lkdj}} \right), \tag{10}$$

and the magnetizing fluxes are

$$\lambda_{mq} = L''_{mq} i_{qs} + \lambda''_q, \tag{11}$$

$$\lambda_{md} = L''_{md} i_{ds} + \lambda''_d. \tag{12}$$

The machine's q- and d-axes rotor dynamics are given by the following ordinary differential equations:

$$p\lambda_{kqj} = -\frac{r_{kqj}}{L_{lkqj}} (\lambda_{kqj} - \lambda_{mq}), \quad j = 1, \cdots, M+1, \tag{13}$$

$$\begin{aligned} p\lambda_{kdj} &= -\frac{r_{kdj}}{L_{lkdj}} (\lambda_{kdj} - \lambda_{md}), \quad j = 1, \cdots, N \\ p\lambda_{fd} &= -\frac{r_{fd}}{L_{lfd}} (\lambda_{fd} - \lambda_{md}) + v_{fd} \end{aligned}. \tag{14}$$

III. Analytical Average-Value Modeling

The analytical approach relates the dc and ac side variables (transferred to a proper qd rotating reference frame) through analytically derived equations for each rectifier mode of operation [17]. For simplicity, the ac variables are transferred to the converter rotating reference frame wherein the averaged d–axis component of the ac input voltage is equal to zero [17]. The ac side of the analytical AVM presented in [17] consists of a three-phase voltage source in series with constant inductances, which is identical to the interfacing circuit of the VBR machine model (see terms $\mathbf{e}''_{abc}$ and L_D in [15]).

The phase current waveforms for the typical rectifier operating mode is shown in Fig. 2, which also depicts the conduction and commutation subintervals with respect to the switching interval T_{sw}. In Fig. 2, a 30-degree firing angle is assumed. The analytical expressions are extracted for both the conduction and commutation subintervals. The dynamic averaging is defined with respect to the prototypical switching interval T_{sw} as

$$\bar{f} = \frac{1}{T_{sw}} \int_{t-T_{sw}}^{t} f(t) dt. \tag{15}$$

where $\bar{f}$ denotes of either the dynamic average voltage or current.

For the first rectifier mode of operation [11], the dc link current $\bar{i}_{dc}$ state equation is defined as

$$\frac{d\bar{i}_{dc}}{dt} = \frac{\frac{3\sqrt{3}}{\pi} v_{asm} \cos\alpha - \left(R_f + \frac{3}{\pi} L_D \omega \right) \bar{i}_{dc} - v_c}{L_f + 2L_D}. \tag{16}$$

The average of ac phase currents in q- and d- axes are calculated for both subintervals as

$$\begin{aligned} \bar{i}^{conv}_{qs} &= \bar{i}^{conv}_{qs,com} + \bar{i}^{conv}_{qs,cond} \\ \bar{i}^{conv}_{ds} &= \bar{i}^{conv}_{ds,com} + \bar{i}^{conv}_{ds,cond} \end{aligned}. \tag{17}$$

where

$$\begin{aligned} \bar{i}^{conv}_{qs,com} = {} & \frac{2\sqrt{3}}{\pi} \bar{i}_{dc} \left[\sin(\mu + \alpha - \frac{5\pi}{6}) - \sin(\alpha - \frac{5\pi}{6}) \right] + \\ & \frac{3}{\pi} \frac{v_{asm}}{L_D \omega} \cos\alpha \left[\cos(\mu + \alpha) - \cos\alpha \right] + \\ & \frac{1}{4} \frac{3}{\pi} \frac{v_{asm}}{L_D \omega} [\cos(2\alpha) - \cos(2\alpha + 2\mu)] \end{aligned}, \tag{18}$$

$$\bar{i}^{conv}_{ds,com} = \frac{2\sqrt{3}}{\pi}\bar{i}_{dc}\left[-\cos(\mu+\alpha-\frac{5\pi}{6})+\cos(\alpha-\frac{5\pi}{6})\right]+$$
$$\frac{3}{\pi}\frac{v_{asm}}{L_D\omega}\cos\alpha\left[\sin(\mu+\alpha)-\sin\alpha\right]+ \quad , \qquad (19)$$
$$\frac{1}{4}\frac{3}{\pi}\frac{v_{asm}}{L_D\omega}\left[\sin(2\alpha)-\sin(2\alpha+2\mu)\right]-\frac{3}{\pi}\frac{v_{asm}}{L_D\omega}\frac{1}{2}\mu$$

$$\bar{i}^{conv}_{qs,cond} = \frac{2\sqrt{3}}{\pi}\bar{i}_{dc}\left[\sin(\alpha+\frac{7\pi}{6})-\sin(\alpha+\mu+\frac{5\pi}{6})\right], \qquad (20)$$

$$\bar{i}^{conv}_{ds,cond} = \frac{2\sqrt{3}}{\pi}\bar{i}_{dc}\left[-\cos(\alpha+\frac{7\pi}{6})+\cos(\alpha+\mu+\frac{5\pi}{6})\right]. \qquad (21)$$

In the above equations, α denotes the thyristor firing delay angle. The commutation angle is calculated as

$$\mu = -\alpha + \arccos\left[\cos\alpha - \frac{L_D\omega\bar{i}_{dc}}{v_{asm}}\frac{2}{\sqrt{3}}\right]. \qquad (22)$$

However, by neglecting the dynamic effect of ac and dc side inductors, the dc and ac side variables of a six-pulse thyristor converter are related by [18]

$$\bar{i}_{dc} = \frac{\frac{3\sqrt{3}}{\pi}v_{asm}\cos\alpha - v_c}{R_f + \frac{3}{\pi}L_D\omega}, \qquad (23)$$

The fundamental component of the ac current can be calculated as

$$I_1 = \frac{\sqrt{2}\left(\frac{3\sqrt{3}}{\pi}v_{asm}\cos\alpha - \frac{3}{\pi}L_D\omega\bar{i}_{dc}\right)\bar{i}_{dc}}{3v_{asm}}. \qquad (24)$$

In the Analytical AVM introduced in [17], the ac side resistance r_D and the steady state voltage drop through the ac side inductance L_D are neglected, which causes inaccuracy when the ac side is weak (low short circuit ratio). Therefore, it is necessary to add the steady-state voltage drop through L_D and r_D to the AVM using

$$\begin{aligned} \bar{v}^{r}_{qs,r_D,L_D} &= L_D\bar{i}^{r}_{ds} + r_D\bar{i}^{r}_{qs} \\ \bar{v}^{r}_{ds,r_D,L_D} &= L_D\bar{i}^{r}_{qs} + r_D\bar{i}^{r}_{ds} \end{aligned} . \qquad (25)$$

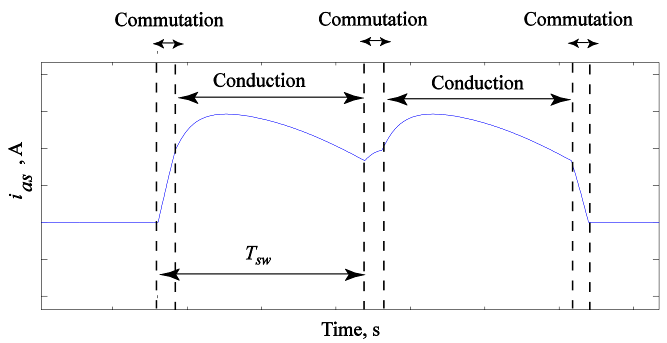

Fig. 2. Typical ac phase current waveform depicting commutation and conduction sub-intervals.

IV. Model Implementation

The block diagram depicting the implementation of the machine/rectifier system AVM is shown in Fig. 3. Direct connection of the machine VBR model to the rectifier AVM that includes the steady-state voltage drop compensation in the ac circuit, introduces multiple algebraic loops, which makes the model implicit and therefore numerical iteration would be required at each time-step. These algebraic loops are illustrated in Fig. 3 by dashed lines. As it is clear from Fig. 3, the causes of algebraic loops can be summarized as follows: First, as it is shown in Fig. 3, the input variables of the rectifier cell are transferred to the converter reference frame for the ease of calculation and vice versa. Then, all the output variables are transferred back to the rotor reference frame. This transformation from rotor to the rectifier reference frame and back is based on the rectifier power angle ϕ which is algebraically calculated based on the input voltages. Second, since the commutation angle μ is calculated algebraically based on the input rectifier voltages, and also used to calculate the rectifier output currents, an algebraic loop is introduced between the inputs and outputs of the rectifier AVM. The introduced algebraic loop causes the numerical iteration and in some cases, MATLAB solvers are unable to solve the simulation. Herein, the algebraic loop in the model is avoided by adding a low-pass filter with a small time constant to the output currents of the rectifier block as it is demonstrated in Fig. 3. This added low pass filter breaks the algebraic loops created due to connection of the machine VBR model to the analytical AVM.

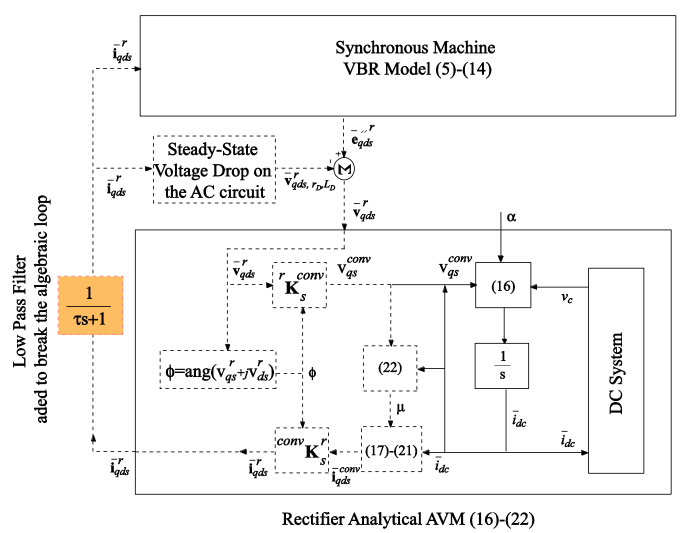

Fig. 3. Implementation of analytical average-value model for synchronous machine/rectifier system.

V. Model Verification

The system shown in Fig. 1 is simulated considering the switching details using ASMG [20] in MATLAB/Simulink [19]. The AVM of the same system, based on the analytical approach (see Section III) and the machine VBR model (see Section II), is also implemented in MATLAB/Simulink using standard library components. For consistency with the previous publications, the system parameters are chosen from a documented configuration presented in [6] and are summarized in Appendix.

The proposed AVM is first validated in steady state by comparing the detailed simulation and the analytical AVM of the machine/rectifier system presented in Fig. 1 for different firing angles. The output dc voltages resulting from the detailed simulation and AVM are presented in Fig. 4. The output dc voltage of the AVM matches very closely the output of the detailed simulation, which validates its accuracy. In order to assess the accuracy of the proposed AVM in following the transient response of the original switching system, a large-signal time-domain transient study is considered. In the following study, the system initially operates in steady state with a constant excitation voltage of 19.5V and a purely resistive dc load of 21Ω. The initial value of the firing angle is set to $\alpha = 30^\circ$. At $t = 0.02$ s, the resistive load is changed to 4.4Ω. The generator field current i_{fd}, along with the dc voltage and current of the detailed simulation and AVM, are shown in Fig. 5. As it can be seen, the AVM follows the transient response of the detailed simulation almost perfectly.

VI. Conclusions

In this paper, an analytical average-value model (AVM) of the synchronous/rectifier system is developed which is explicit and thus computationally more efficient than the previous implicit AVMs. Here, the voltage-behind-reactance (VBR) machine model with constant parameters is directly interfaced with the rectifier AVM. The validity of the new model is demonstrated in steady state and during transients by comparing it to the detailed simulation. In particular, the AVM is shown to yield very accurate steady-state dc voltages over the whole range of thyristor firing angles. The AVM is also shown to follow very closely the detailed simulation transients during a load step change.

The accuracy of the proposed average-value model is established by comparing its performance to the detailed simulation for different loading conditions, and transients in extended range of operating conditions.

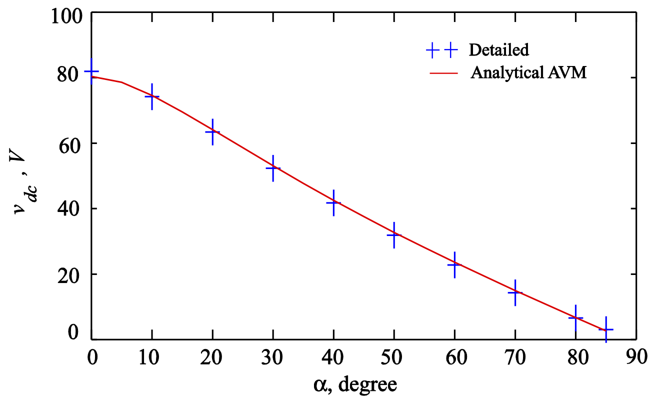

Fig. 4. Steady state output dc voltage versus the thyristor firing angle.

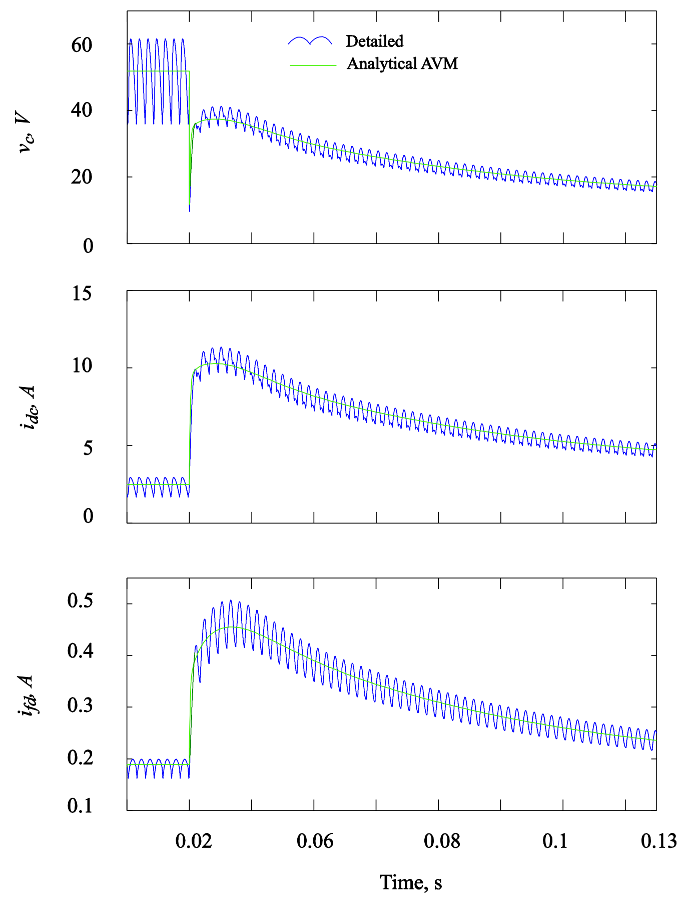

Fig. 5. Transient response to a step change in load.

VII. Appendix

Synchronous machine parameters: US Electrical Motors, 5 HP, 230Volt, 215T Frame, 1800 rpm, rated field current 1.05A, custom-made for university lab.

$\omega_b = 2\cdot\pi\cdot 60\,\text{rad/s}$	$P = 4$ (four poles)
$r_s = 0.382\,\Omega$	$x_{ls} = 0.4222\,\Omega$
$x_{mq} = 9.3871\,\Omega$	$x_{md} = 14.8158\,\Omega$
$r'_{kq1} = 5.07\,\Omega$	$x'_{lkq1} = 1.3195\,\Omega$
$r'_{kq2} = 1.06\,\Omega$	$x'_{lkq2} = 1.3195\,\Omega$
$r'_{kq3} = 0.447\,\Omega$	$x'_{lkq3} = 9.8772\,\Omega$
$r'_{kd1} = 140\,\Omega$	$x'_{lkd1} = 3.7209\,\Omega$
$r'_{kd2} = 1.19\,\Omega$	$x'_{lkd2} = 1.8510\,\Omega$
$r'_{kd3} = 1.58\,\Omega$	$x'_{lkd3} = 1.7002\,\Omega$
$r'_{fd} = 0.112\,\Omega$	$x'_{lfd} = 0.5768\,\Omega$
stator-to-field turns ratio	$N_s/N_{fd} = 0.0269$

Dc link filter parameters:
$L_f = 1.19\,\text{mH}$; $r_f = 0.32\,\Omega$; $C_f = 2.28\mu\text{F}$.

VIII. References

[1] H. A. Peterson and P. C. Krause, "A direct- and quadrature- axis representation of a parallel ac and dc power system," *IEEE Trans. Power App. Syst., vol. 85, no. 3, pp. 210-225, Mar. 1966.*

[2] P. C. Krause and T. A. Lipo, "Analysis and simplified representation of a rectifier-inverter induction motor drive," *IEEE Trans. Power App. Syst., vol. 88, no. 5, pp. 588-596, May 1969.*

[3] S. D. Sudhoff and O. Wasynczuk, "Analysis and average-value modeling of line-commutated converter-synchronous machine systems," *IEEE Trans. Energy Convers., vol. 8, no. 1, pp. 92-99, 1993.*

[4] S. D. Sudhoff, "Analysis and average-value modeling of line-commutated converter\\\—synchronous machine systems," *IEEE Trans. Energy Convers., vol. 8, no. 3, pp. 408-410, Mar. 1993.*

[5] H. Zhu, "New multi-pulse diode rectifier average models for ac and dc power systems studies," PhD Dissertation, Virginia Polytechnic Institute and State University, 2005.

[6] S. D. Sudhoff, K. A. Corzine, H. J. Hegner, and D. E. Delisle, "Transient and dynamic average-value modeling of synchronous machine fed load-commutated converters," *IEEE Trans. Energy Convers., vol. 11, no. 3, pp. 508-514, Sep. 1996.*

[7] J. T. Alt, S. D. Sudhoff, and B. E. Ladd, "Analysis and average-value modeling of an inductorless synchronous machine load commutated converter system," *IEEE Trans. Energy Convers., vol. 14, no. 1, pp. 37-43, Mar. 1999.*

[8] M. Shahnazari, A. Vahedi, "Improved dynamic average value modeling of brushless excitation system in all rectification modes," *IET Electr. Power Appl., Vol. 4, Iss. 8, pp. 657–669, Sep. 2010.*

[9] I. Jadric, D. Borojevic, and M. Jadric, "A simplified model of a variable speed synchronous generator loaded with diode rectifier," *in Proc. IEEE Power Electronics Specialists Conf. (PESC) , 1997, pp. 497-502.*

[10] I. Jadric, D. Borojevic, and M. Jadric, "Modeling and control of a synchronous generator with an active dc load," *IEEE Trans. Power Electron., vol. 15, no. 2, pp. 303-311, Mar. 2000.*

[11] J. Jatskevich, S. D. Pekarek, and A. Davoudi, "Parametric average-value model of a synchronous machine-rectifier system," *IEEE Trans. Energy Convers., vol. 21, no. 1, pp. 9-18, Mar. 2006.*

[12] J. Jatskevich, S. D. Pekarek, and A. Davoudi, "Fast procedure for for constructing an accurate dynamic average-value model of synchronous machine-rectifier system," *IEEE Trans. Energy Convers., vol. 21, no. 2, pp. 435-441, Jun. 2006.*

[13] S. Chiniforoosh, J. Jatskevich, A. Yazdani, V. Sood, V. Dinavahi, J. A. Martinez, and A. Ramirez, "Definitions and Applications of Dynamic Average Models for Analysis of Power Systems," *IEEE Trans. Power del., vol. 25, no. 4, pp. 2655-2669, Oct. 2010.*

[14] S. Chiniforoosh, H. Atighechi, A. Davoodi, J. Jatskevich, A. Yazdani, S. Filizadeh, M. Saeedifard, J. A. Martinez, V. Sood, K. Strunz, J. Mahseredjian, V. Dinavahi, "Dynamic Average Modeling of Front-End Diode Rectifier Loads Considering Discontinuous Conduction Mode and Unbalanced Operation," *IEEE Trans. Power del., vol. 27, pp. 421-429, Jan. 2011.*

[15] M. Chapariha, L. Wang, J. Jatskevich, H. W. Dommel, S. D. Pekarek, "Constant-Parameter R-L-Branch Equivalent Circuit for Interfacing AC Machine Models in State-Variable-Based Simulation Packages," *IEEE Trans. Energy Convers., vol. 27, no. 3, pp. 634-645, Sep. 2012.*

[16] S. D. Pekarek, E. A. Walters, "An accurate method of neglecting dynamic saliency of synchronous machine in power electronic based systems," *IEEE Trans. Energy Convers., vol. 14, no. 4, pp. 1177-1183, Dec. 1999.*

[17] P. C. Krause, O. Wasynczuk, and S. D. Sudhoff, Analysis of Electric Machinery and Drive Systems, 2nd Edition, IEEE Press, Piscataway, NJ, 2002.

[18] G. Seguier, Power Electronic Converters, 2nd Edition, McGraw-Hill Book Company, 1986.

[19] "Simulink Dynamic System Simulation Software, Users Manual, "MathWorks Inc., 2008. [Online]. Available: http://www.mathworks.com.

[20] Automated State Model Generator (ASMG) Reference Manual, P. C. Krause and Associates, Inc., West Lafayette, IN, USA, 2002.